MECHANIKA TEORETYCZNA
I STOSOWANA
Journal of Theoretical
and Applied Mechanics
4, 30, 1992

EXPERIMENTAL DETERMINATION OF CRITICAL STRESSES IN SANDWICH CYLINDERS UNDER NON-ELASTIC CONDITIONS

FRANCISZEK ROMANÓW

Zielona Góra Engineering Institute

In the present paper both the theoretical analysis of the compression process acting upon cylinders filled with the polyurethanes and the results of experiments have been presented. The experimental tests were performed under substantial plastic strains until the cylinder totally collapsed. Depending on the test bar slenderness ratio different strain patterns have been obtained. It is noteworthy that the critical compressive stresses curve obtained for the mean slenderness ratios neither coincides with the Tetmajer–Jasiński straight line nor with the Johnson–Ostenfeld parabola. A relatively simple function approximating the experimental results has been presented.

1. Introduction

Modern designs and instruments have to meet strict requirements. They should display, for example, high strenght or stiffness, be of light weight and the manufacture and exploitation costs of them should be relatively low. Some subassemblies should also meet certain additional requirements, like e.g. the maximal energy absorption condition imposed on the buffers and other shock absorbers.

One should expect that these requirements can be most effectively satisfied by means of the modern sandwich designs application.

The high strenght and stiffness requirement together with the deep energy absorption condition imposed on the thin-walled designs could be satisfied by means of e.g. the continuous support with the aid of the polyurethanes foam layer. One can also make the construction materials more useful by applying accurate calculation methods basing e.g. on the physical nonlinearity theory. In the case of buffers one should take into account, for example, the substantial plastic strain. The theory of design analysis by means of the complete plastic conditions application has recently become an interesting subject of many theoretical and experimental researches. The analysis and experimantal results obtained for circular sandwich bars

of different lengths filled with the polyurethanes foam and subject to the compression are given in the present paper. The theoretical analysis of critical compressive stresses in slender bars was given by Romanów [2], while the same problem in sandwich shells was considered by Dzielendziak and Romanów [3]. The kinematic analysis of energy absorption in hollow, rectangular columns under compression was shown by Abramowicz [3]. One can also find some solutions to different stability problems in inelastic regions of thin-walled designs in the work of Królak et al. [4].

2. Experimental tests

The tests were carried out on circular tubes of external diameter 30 mm and with the walls 0.75 mm thick made of duraluminium PA-4N-tb according to the Polish Standard PN-7-/H-74592. The following material properties were taken according to experiments: $E = 72387$ MPa; $R_H = 153$ MPa; $R_{0.2} = 191$ MPa; $R_m = 259$ MPa; $A_{10} = 19.8\%$.

The cores were made of polyurethanes foam of densities: $\rho_r = 100, 125, 150$ kg/m^3, respectively; the coefficients applied were: Poisson ratio $\nu_r = 0$; Kirchoff modulus $G_r = 19.4$ MPa; Young modulus $E_r = 38.8$ MPa.

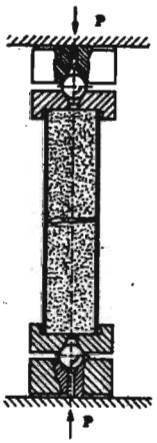

Fig. 1.

The test bar slenderness ratios were calculated for hollow tubes and were equal to: 4.7; 5.8; 6.8; 7.7; 9.5; 20; 50; 75, respectively.

For the more exact determination of the test bar carrying capacity in the plastic region the number of samples of small slenderness ratio was increased.

The test bars of slenderness ratio $\lambda \geq 20$ were compressed with the aid of sharing shackles (Fig.1), while the remaining samples were compressed on the testing machine directly between the holders.

The results obtained for tubes filled with the polyurethane foam were compared to those obtained for the hollow samples under the same conditions. 51 tubes were tested i.e. 23 hollow and 28 filled with polyurethane foam ones. The results for hollow tubes are presented in Table 1, while those obtained for the filled ones can be found in Tables 2 and 3, respectively.

Table 1. Critical loadings and deformation works obtained for the hollow tubes

No.	Notation	a [mm]	λ	P_{cr} [kN]	P_{1m} [kN]	σ_{cr} [MPa]	σ_{1m} [MPa]	L_1 [J]	L_{1m} [J]	The form of deform.
1	1 p	50	4,8	15	15	217	217			
2	9 p	60	5.8	14.8	14.8	214	214	218		
3	12 p			14.1		205		17.3		
4	13 p			14.3		207		18.8		
		70	6.8		14.3		207		17.9	Fig.6
5	14 p			14.1		205		17.5		
6	15 p			14.1		213		18.0		
7	17 p			15.1		227		22		
		80	7.8		15.2		220		18.0	Fig.6
8	18 p			14.7		213		14.1		
9	21 p			15.1		219		25		
10	22 p	99	9.6	14.5	14.8	210	214	21.2	22.4	Fig.6
11	23 p			14.7		213		20.9		
12				13.3		193		27		
13				13.6		197		28		
		206	20		13.7		198		22.3	Fig.8
14				14.0		203		16		
15				13.9		202		18		
16				11.8		171		13.7		
17				11.1		161		12.0		
		515	50		11.5		168		12.8	Fig.8
18				10.1		146		11.2		
19				12		174		14.5		
20				8.8		128		8.6		
21				8.8		128		8.3		
		772	75		8.7		125		8.3	Fig.8
22				7.8		113		6.7		
23				9.3		134		9.6		

2.1. Disscussion of the tests carried out in elastoplastic conditions

Below, one can find some remarks concerning hollow tubes. The results obtained in experiments for slenderness ratios $4.8 \leq \lambda \leq 75$ are given in Table 1.

The following notation is used in figures and tables, respectively

- a – tube length,
- λ – slenderness ratio,
- P_{cr} – maximal force which the tube is able to carry, $P_{cr} = P_1$, corresponding to the point 1 in Figs.2 and 4,
- σ_{cr} – stresses which one can calculate dividing the critical force P_{cr} magnitude by the hollow tube cross-section area; $\sigma_{cr} = \sigma_1$,
- L_1 – work of deformation corresponding to the area under the 0–1 segment of the curve,
- L_c – total work of deformation,
- k_{p1} – ratio between the same P_1 force for the hollow and filled tube, respectively,
- k_{L1} – the same as the foregoing ratio but corresponding to the work of deformation,
- k_{Lc} – coressponds to the total work of deformation.

For the tested hollow samples the limiting slenderness ratio λ_{lim} calculated with the aid of the Euler formula (for $R_H = 155$ MPa) equals 68.3.

The control tests carried out for hollow tubes of $\lambda = 75$ (Table 1) have shown a very good corelation between the experimantal test results and those obtained after theoretical calculations, e.g. σ_{cr} from experiments was equal to 125 MPa, while after calculation one can obtain 127 MPa. For samples of renderness $\lambda = 75$ the critical compressive stresses have not reached the limit of proportionality, which for the present material is equal to $R_H = 153$ MPa. The values of critical compressive stresses obtained for the tubes of the slenderness ratio $\lambda = 20$ have been lying in the range between $R_H = 153$ MPa and $R_{0.2} = 191$ MPa. The neglegible differences have appeared between the values of the critical compressive stresses in tubes of $\lambda_{lim\,1} \leq 10$, which were lying in the range of $207 \div 220$ MPa. The mean value has been calculated as 214 MPa with the standard deviation equal to 4.8.

The experimental results concerning the critical compressive stresses in samples of slenderness ratio

$$10 \leq \lambda \leq \lambda_{lim} = 68.3$$

have been approximated by means of the Tetmajer straight line (Fig.3)

$$\sigma_{cr} = 226.4 - 1.1\lambda \tag{2.1}$$

while the value of 214 MPa has been applied to the samples of $\lambda < 10$.

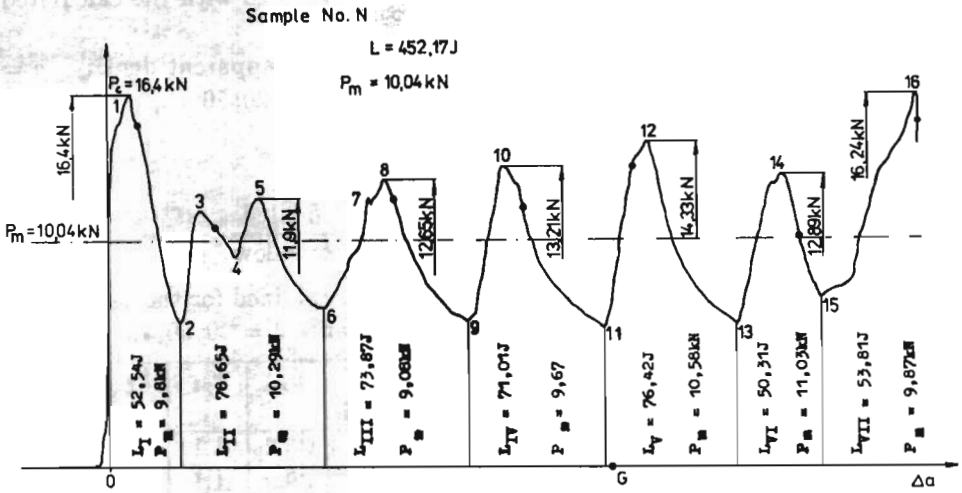

Fig. 2.

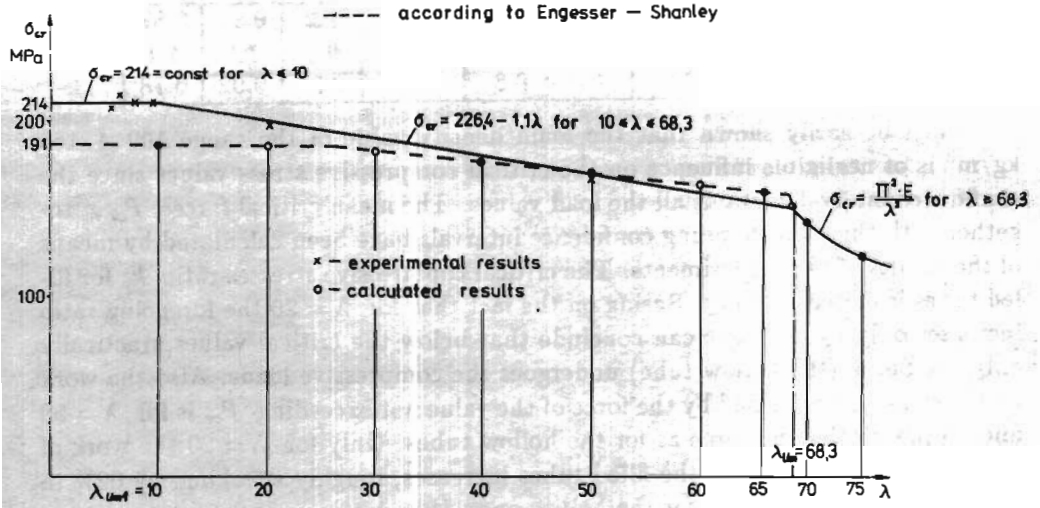

Fig. 3. The critical compressive stresses diagram versus the slenderness ratio how the hollow tubes

The Euler formula holds for $\lambda \geq \lambda_{lim} = 68.3$.

The whole diagram of the critical compressive stresses distribution in hollow tubes versus the slenderness ratio is shown in Fig.3 together with the results obtained with the aid of the Engesser–Shanley theory (broken line). It can be easily seen from Fig.3 that the experimental results do not corespond to with the calculated ones.

The results for tubes filled with the polyurethanes of apparent density $\rho = 100; 125; 150$ kg/m^3, respectively of slenderness ratio $\lambda = 20; 50; 75$, respectively are presented in Table 2.

Table 2 contains also the following additional notations

$$k_p = \frac{P_{cr}\,\text{filled}}{P_{cr}\,\text{hollow}} \qquad K_{LC} = \frac{L\,\text{filled}}{L\,\text{hollow}} \tag{2.2}$$

Table 2. Critical loadings and deformation works obtained for the tubes filled with foams of different densities for the slenderness ratio $\lambda = 20; 50; 75$

No.	ρ [kg/m^3]	λ	$P_{cr\,m}$	Confidence interval P_{cr}	$\sigma_{cr\,m}$ [MPa]	L_m	k_{pl}	k_{LC}
24	100		14.6	1.4 ÷ 5.2		35.2	1.1	1.56
25	125	20	14.4	12.6 ÷ 16.3	211	39.9	1.1	1.33
26	150		14.2	12.7 ÷ 15.7		33.3	1.1	1.48
27	100		11.6	10.5 ÷ 12.7		12.9	1.01	1.01
28	125	50	11.5	10.1 ÷ 12.8	167	13.3	0.99	1.04
29	150		11.2	10.8 ÷ 11.6		12.2	0.97	0.95
30	100		7.8	7.04 ÷ 8.6		7.2	0.94	0.87
31	125	75	9.0	6.47 ÷ 11.6	118	9.0	1.1	1.1
32	150		7.6	6.4 ÷ 8.8		6.58	0.92	0.78

It can be easily shown that the foam density value of the range 100 ÷ 150 kg/m^3 is of negligible influence on the critical compressive stress values since the confidence interval contains all the load values. The mean critical forces $P_{cr\,m}$ together with the corresponding confidence intervals have been calculated by means of the results of four experiments. The critical copmressive stresses ratio k_p for filled tubes is closed to unity. Basing on the fact that for $\lambda = 20$ the foregoing ratio increases only by 10% one can conclude that below the critical values,practically only the lining (the hollow tube) undergoes the compressive loads. Also the work of deformation performed by the force of the value not exceeding P_{cr} is for $\lambda = 50$ and 75 practically the same as for the hollow tubes. Only for $\lambda = 20$ the work of deformation performed on the filled tubes increases, roughly speaking, by 62% in comparison with the value for the hollow ones ($k = 1.46$).

The diagrams of compression for samples of $\lambda \geq 20$ are presented in Fig.4. It can be easily seen that particular curves differ from each other depending on the slenderness ratio values. For larger values of slenderness ratio the stability loss

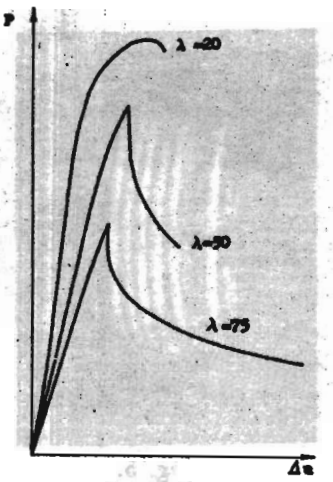

Fig. 4.

arrives in "an instant way", shown by the refraction of the diagrams through the smaller angle. For slenderness ratio $\lambda = 20$ the sample deforms in a milder way. It is noteworthy that in all three diagrams there exist the region of proportionality between the compression force and the compression. Calculations of bars of this type were given by Romanów [1].

2.2. Discussion of the plastic conditions

The way of sample crushing in the form of "bellows" is characteristic in this case.

Depending on the size, the samples deform in the form of

- ring on the circle diagram (Fig.5),
- fold on the hexagon projection (Fig.6),
- in the mixed form in such away that some folds are of the ring form, while the rest of them takes the form of hexagon (Fig.7).

These patterns of deformation are called: ring, hexagon and ring–hexagon ones, respectively.

The samples of the small slenderness ratio values have deformed in such a way according to the results shown in Fig.3. For larger values of the slenderness ratio, after the loss of stability the samples have broken in one cross–section only (cf Fig.8).

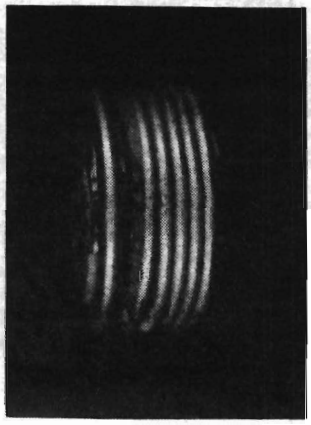

Fig. 5.

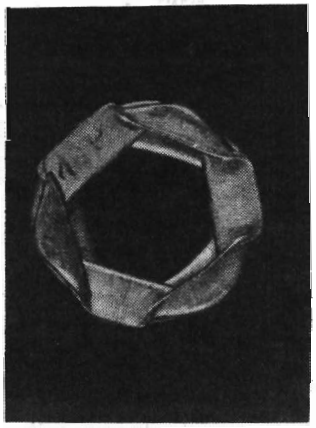

Fig. 6.

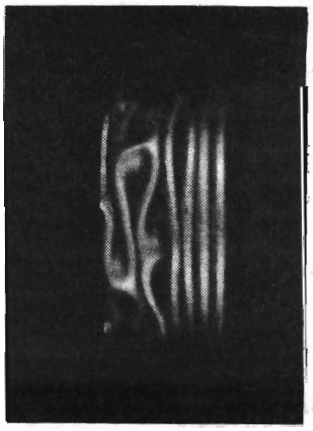

Fig. 7.

Fig. 8.

According to the experimental results it can be seen that samples of the "higher stiffness" tend to the ring pattern of deformation.

Having two samples of the same slenderness ratio it can be found that the hollow one deforms in the hexagon pattern, whole the filled tube deformation patterns on the ring.

Let us have a look at the diagram shown in Fig.2 (test bar No.37, Table 3) being the typical one for all the samples of the series from No.33 to No.51 (Table 3), i.e. for $\lambda < 10$. The plot of the compressing force P [kN] versus the sample shortage Δa is presented. Having the initial length $a = 60$ mm and the final one $a_1 = 15$ mm, respectively one can, after a simple calculation, obtain the sample shortage being the distance from the origin to the point 16 in the abscissa direction since the accepted abscissa scale is 5:1 and the real distance equals to 225 mm. The deformation is equal $\varepsilon = \Delta a/a = -0.75$.

After passing the point 1 corresponding to the maximal force $P_1 = 16.4$ kN which the sample can undergo it begins to lose the stability. The first half-wave arrives on one end at $\sigma_1 = 238$ MPa which is in fact one of the lowest stresses in the whole group of the tubes, calculated with regard to the hollow tube cross-section only (the core was neglected). Taking the small value of the Young modulus for the core ($E_r = 38.8$ MPa) into account one can establish the fact that the whole load is carried by the hollow tube, since the force which the core undergoes equals 0.0814 kN.

It is noteworthy that the values of these stresses lie in the region between the yield strength $R_{0.2} = 191$ MPa and the ultimate strength $R_m = 259$ MPa. Basing on the results presented in Table 3 one can calculate the mean stress for this group of samples $\sigma_m = 245$ MPa.

The stress σ_1 one should take for the critical one corresponding to the moment of the first half-wave occurence. It is the maximal stress the sample can undergo.

The diagram shows that the maximal forces corresponding to the points 5, 8, 10, 12 and 14, respectively do not exceed the value of P_1. The differences between

Table 3. Results for filled tubes of slenderness ratio $\lambda < 10$

No.	Notation	a [mm]	λ	P_{cr} [kN]	P_{1m} [kN]	σ_{cr} [MPa]	σ_{1m} [MPa]	L_1 [J]	L_{1m} [J]	L_c [J]	L_{cm} [J]	k_{p1}	k_{L1}	k_{Lc}	ρ [kg/m^3]
33	1C1			16.2		234		13.9							
34	2C1			17.2		248		20.4		438					
		48	4.7		16.9		245		17.9		380				150
35	3C1			17.1		247		19.4							
36	4C1			17.0		245		17.9		322					
37	N			16.4		238									
		60	5.8		16.9		245		17.9			1.14		3.1	
38	B3			17.5		254		17.5							
39	8B3			16.8		244				415					
40	7B3			17.2		250				552					125
41	3B3			17.2		248		25.1		575				3.4	
42	4B3	70	6.8	17.1	17.2	247	249	25.3		530		1.2	1.03		
43	5B3			16.5		239		18.1		523					
44	1C3			17.3		250		23.2		523					
45	2C3			18.2		264		31.1							150
46	19P			15.6		226				426			1.3	3.7	
47	1A4	80	7.7	17.5	16.7	253	242	26		589		1.1			100
48	2A4			16.9		244		22							
49	1E7			16.1		233		27.3							
50	2E7	98	9.5	16.7	16	242	234	34		547		1.1	1.23	3.9	
51	3E7			15.5		245		21.2							

the succesive maximal force are relatively small with the mean value equal to $P_{m5} \cong 13$ kN.

The ratio between the force $P_1 = P_{max}$ and the mean one P_{m5} causing the succesive half-wave equals to 1.26. The compression tests were stopped at the point 16, corresponding to the deformation level at which all the halfwaves were completely compressed and the contact appear. The forces at points 1 and 16, respectively correspond to each other.

The compressed bellows could possibly stand for the homogeneous material (the new tube of thick wallls), but the experiments were stopped at this point.

The total work of deformation (the proper area below the curve 0,1,2,...,16) equals 452.2 J. The mean work of deformation corresponding to one half-wave is equal to 65 J. The mean compressive force for the total work of deformation is equal to $P_{mt} = 10.04$, thus their ratio P_1/P_{mt} eqals 1.64. It can be seen (Fig.3) that starting from the point 8 the appropriate segments of the curve pass in a regular way. The additional extrema arriving at points 3,4 and 7, respectively are situated between points 2 and 5 or 6 and 8 only.

Applying the diagram presented in Fig.9 one can easily explain this effect.

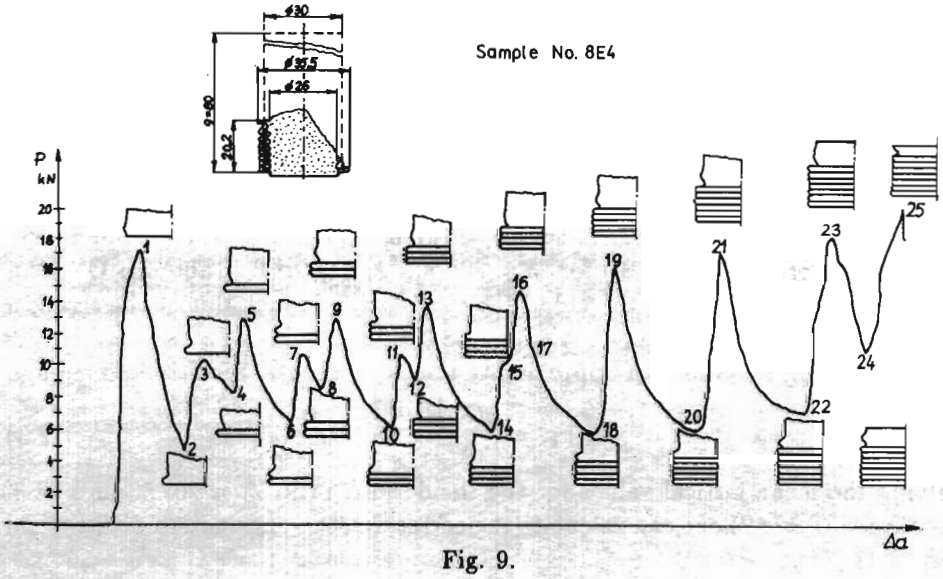

Fig. 9.

In this figure the points 1,2,... and 25, respectively are assigned to the deformed sample.

The first tube blister arrives at the point 1. After the first half-wave complete forming the force decreases to the point 2, at which the first half-wave remains incompressed. At the point 2 a concavity arrives which become deeper and deeper

till; the force reaches the point 3. When the force decreases to the point 4 the first tube blister becomes hold down, while the concavity remains almost udeformed.

At point 5 another tube blister arrives and the course begins to repeat, so at the pont 8 one can see two strongly compressed blisters together with the concavity. This way of the blister forming continues to the point 16.

This region is characteristic, since for one blister shaped enough and one new concavity to arrive (on the diagram – force versus shortage) one should pass through the two half–waves, i.e. through the points 0,1,2 and 2,3,4, respectively. For one half–wave to create one should pass through the two minima (points 2 and 4, respectively) and through the two maxima (points 1 and 3, respectively). The similar process repeats till the point 16 is reached.

Starting from point 16 there is one–to–one correspondence between the the tube blister and the half–wave on the diagram.

It is noteworthy that the force necessary for the next blister to accur on the test bar should be, roughly speaking, greater than the previous one $P_{25} > P_{23} > \ldots$ and so on.

The characteristic swings of the curve which can be seen in the segments 3–4, 7–8 and 11–12, respectively vanish at point 15 and the next half–waves (starting from the pont 16) are already smooth.

The experimental test results for the critical compressive stresses (denoted in Fig.10 by crosses) can be easily divided into three groups. For the small values of slenderness ratio $\lambda < 10$, the stresses obtained are of the values close to each other with the mean value equal to 245 MPa while the standard deviation about it equals 8.5. The experimental results for this group of tubes are given in Table 3.

Neither the Tetmajer straight line nor the Jahnson curve overlap the measurements results (crosses in Fig.10) for $\lambda = 20;\ 50;\ \lambda_{lim} = 68.3$ (Table 2). One can approximate the results with the aid of the curve being in fact almost the straigth line ($\sigma_{cr} = 188.6 - 0.492\lambda$, for $\lambda = 43.8 \div 68.3$).

The following function can approximate the experimental results close enough

$$\sigma_{kr} = \frac{b(\lambda)E}{\lambda^2} \tag{2.3}$$

Applying the mean critical values for the slenderness ratio $\lambda = 20;\ 50$ and 68.3, respectively (Table 2) one can calculate the corresponding parameters with the aid of Eq (2.3)

$$\begin{aligned} b_{20} &= \frac{\sigma_{cr20}\lambda_{20}^2}{E} = \frac{211 \cdot 20^2}{72387} = 1.16 \\ b_{50} &= \frac{167 \cdot 50^2}{72387} = 5.7 \\ b_{68.3} &= \frac{153 \cdot 68.3^2}{72387} = 9.8 \end{aligned} \tag{2.4}$$

where $\sigma_{cr68.3} = 153$ MPa represents the Eulerian stresses calculated for the limiting slenderness ratio $\lambda_{lim} = 68.3$. Relative to the $b_i - \lambda$ coordinate system one can approximate these values by means of the following parabola

$$a_i = c\lambda^2 + d\lambda \tag{2.5}$$

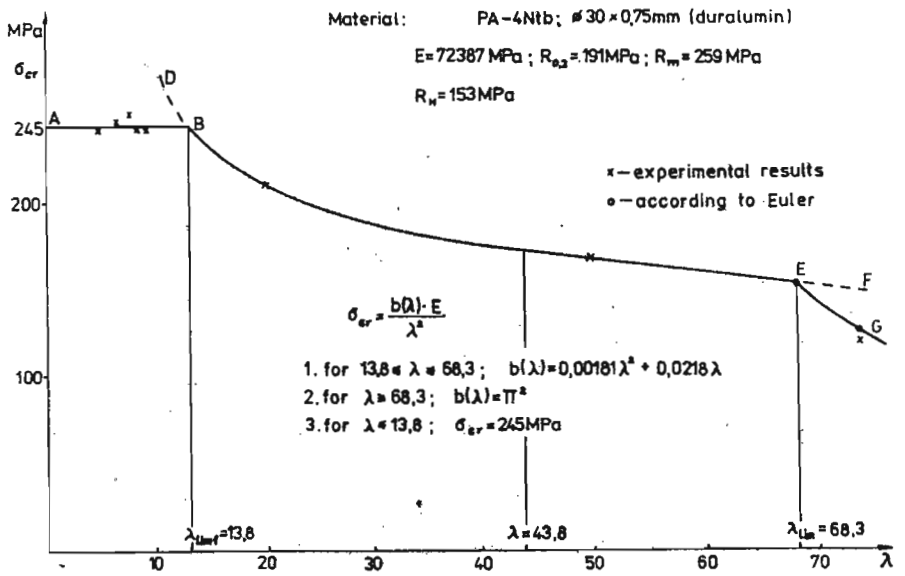

Fig. 10.

Calculating the parameters c and d in terms of the corresponding values of a_i and λ_i one obtains

$$b = 0.00181\lambda^2 + 0.0218\lambda \tag{2.6}$$

The final form of the function approximating the critical compressive stresses distribution in filled tested tubes $(13.8 \leq \lambda \leq 68.3)$ is as follows

$$\sigma_{cr} = \frac{(0.00181\lambda^2 + 0.0218\lambda)E}{\lambda^2} \tag{2.7}$$

We can assume that the expression

$$\frac{(0.00181\lambda^2 + 0.0218\lambda)E}{\lambda^2} \tag{2.8}$$

stand for the equivalent Young modulus. The formula for the critical compressive stresses takes then the well-known form

$$\sigma_{cr} = \frac{\pi^2 E_z}{\lambda^2} \tag{2.9}$$

The DBEF curve in Fig.10 represents the graph of the foregoing formula. The Eulerian hiperbola bounds this curve from the right–hand side (point E). The slenderness ratio corresponding to the point E stands for the limiting slenderness ratio λ_{lim} according to the Eulerian formula application limits for the testing tubes and for $R_H = 153$ MPa, $\lambda_{lim} = 68.3$.

For the small values of slenderness ratio ($\lambda \leq 10$) one can assume the critical compressive stresses to be constant and equal to 245 MPa. This is the reason why the AB straight line crosses the curve at the point B, being the bounding point of the DF curve application from the left–hand side. The limiting slenderness ratio $\lambda_{lim\,1} = 13.8$ corresponds to the point B. The BE curve approximates the experimental results close enough since the maximal deviation about it does not exceed the value of 2.4%.

Eq (2.7) can be rewritten as

$$\sigma_{cr} = \left(0.00181 + \frac{0.0218}{\lambda}\right) E \tag{2.10}$$

Assuming that the critical compressive stresses are proportinal to the yield point, the foregoing formula can be generalized to the form valid for the different duraluminium materials:

$$\sigma_{cr} = \left(0.00181 + \frac{0.0218}{\lambda}\right) \frac{1.2827 \cdot R_{0.2}}{245} E \tag{2.11}$$

$$\sigma_{cr} = \left(9.48 + \frac{114}{\lambda}\right) \cdot 10^{-6} E R_{0.2} \tag{2.12}$$

References

1. ROMANÓW FR., DZIELENDZIAK S., 1988, *Stateczność opsiowo ściskanych cylindryczneych powłok dwuwarstwowych*, Mech.Teoret.i Stos., 3, 26
2. DZIELENDZIAK S., ROMANÓW FR., 1989, *Festigkeit azial gedrückter zylindrischer Sandwichelemente unter Berücksichtigung nichtlinearer Verformbeikart des Kerns*, Techn.Hochschule Zwickau, Wissenschaftliche Berichte, Aktive und Passive Sicherheit des Kraftfarzeuges
3. ABRAMOWICZ W., 1979, *Kinematyczna analiza energochłonności cienkościennych kolumn metalowych*, Prace IPPT, 19, Warszawa
4. KRÓLAK M., 1990, *Stany zakrytyczne i nośność graniczna cienkościennych dźwigarów o ścianach płaskich*, PWN Warszawa–Lódź
5. ROMANÓW FR., 1989, *Zur Stabilität von Sandwichkonstruktionen*, Techn. Universität, Dresden
6. ROMANÓW FR., 1983, 1984, *Hyperbolischer dreiaxialer Verschiebungszustand von flachen Sandwichkonstruktionen und schwachgewölbten Sandwichschalen*, Bauingenieur 58, Bauingenieur 59

Naprężenia krytyczne warstwowych cylindrów w stanach niesprężystych. (Badania doświadczalne)

Streszczenie

W pracy przedstawiono wyniki badań i analizę ściskanych cylindrów wypełnionych poliuretanem. Badania prowadzono przy dużych odkształceniach plastycznych, aż do całkowitego zgniecenia cylindrów. W zależności od smukłości próbek otrzymano różne formy odkształceń. Charakterystycznym jest to, że dla średnich smukłości krzywa naprężeń krytycznych różni się od prostej Tetmajera–Jasińskiego i od paraboli Johnsona–Ostenfelda.

Przedstawiono stosunkowo prostą funkcję, która bardzo dobrze aproksymuje wyniki badań.

Manuscript received January 7, 1991; accepted for print March 25, 1992